



ANISOTROPY AND SIZE EFFECTS IN $\text{Bi}_{1-x}\text{Sb}_x$ SEMICONDUCTOR WIRES IN A MAGNETIC FIELD

Albina A. Nikolaeva^{1*}, Leonid A. Konopko¹, Tito E. Huber^{2**}, Ivan A. Popov¹,
Pavel P. Bodiul¹, and Gheorghe Para¹

¹*Ghitu Institute of Electronic Engineering and Nanotechnology, str. Academiei 3/3, Chisinau MD-2028 Republic of Moldova*

**E-mail: a.nicolaeva@nanotech.md*

²*Howard University, Department of Chemistry, Washington, United States*

***E-mail: titoehuber@gmail.com*

(Received November 29, 2021)

<https://doi.org/10.53081/mjps.2021.20-2.01>

CZU:533.9+538.9+539.1/.2+544

Abstract

The electron transport and longitudinal and transverse magnetoresistance (MR) of glass-insulated $\text{Bi}_{0.92}\text{Sb}_{0.08}$ single-crystal wires with diameters of 180 nm to 2.2 μm and the (1011) orientation along the wire axis have been studied. The wires have been prepared by liquid-phase casting. It has been first found that the energy gap ΔE increases by a factor of 4 with a decrease in wire diameter d due to the manifestation of the quantum size effect, which can occur under conditions of a linear energy–momentum dispersion law characteristic of both the gapless state and the surface states in topological insulators (TIs). It has been revealed that, in strong magnetic fields at low temperatures, a semiconductor–semimetal transition occurs, which is evident as an anomalous decrease in the transverse MR anisotropy and the appearance of a metallic temperature dependence of resistance at $T < 100$ K. It has been found that the effect of negative MR, the appearance of an anomalous maximum in the longitudinal MR, and the dependence of $H_{\text{max}} \sim d^{-1}$ at 4.2 K is a manifestation of the classical MacDonald–Chambers size effect. The calculated value of the p_F^\perp component of the Fermi momentum perpendicular to the magnetic induction vector H is 2 times higher than the p_F^\parallel value for pure bismuth wires. The features of the manifestation of the quantum size effect in $\text{Bi}_{0.92}\text{Sb}_{0.08}$ wires, semiconductor–semimetal electronic transitions induced by a magnetic field, and a decrease in the transverse MR anisotropy indicate the occurrence of new effects in low-dimensional structures based on semiconductor wire TIs, which require new scientific approaches and applications.

Keywords: semiconductor nanowires, size effects, topological insulator, anisotropy, magnetoresistance, electronic transitions

Rezumat

A fost studiat transportul de electroni și magnetoresistența longitudinală și transversală (MR) a firelor monocristaline de $\text{Bi}_{0.9}\text{Sb}_{0.08}$ în înveliș de sticlă cu diametre de la 180 nm până la 2,2 μm și orientarea (1011) de-a lungul axei firului. Firele au fost obținute prin turnarea din faza

lichidă. Pentru prima dată s-a constatat că ΔE crește de 4 ori cu micșorarea diametrului firului d , datorită manifestării efectelor cuantice dimensionale, care pot apărea în condițiile unei legi de dispersie energie-impuls liniare, care este caracteristică atât pentru o stare fără gap , cât și pentru stările de suprafață în izolatorii topologici (TIs). S-a observat că, în câmpurile magnetice puternice la temperaturi scăzute, se produce o tranziție semiconductor-semimetal, care se manifestă printr-o scădere anormală a anizotropiei magnetoresistenței transversale și apariția unei dependențe metalice de temperatură a rezistenței la $T < 100\text{K}$. S-a constatat că efectul magnetoresistenței negative, apariția unui maxim anormal în magnetoresistența longitudinală și dependența $H_{\text{max}} \sim d^{-1}$ la 4,2 K sunt o manifestare a efectului dimensional clasic MacDonald-Chambers. Valoarea calculată a componentei p_F^\perp a impulsului Fermi, perpendicular pe vectorul de inducție magnetică H , este de 2 ori mai mare decât valoarea p_F^\parallel pentru firele de bismut pur. Particularitățile manifestării efectului cuantic dimensional în firele $\text{Bi}_{0,92}\text{Sb}_{0,08}$, tranzițiile electronice semiconductor-semimetal induse de un câmp magnetic și scăderea anizotropiei magnetoresistenței transversale indică la manifestarea de noi efecte în structurile de dimensiuni reduse ale izolatorilor topologici pe fire semiconductoare, care necesită noi abordări științifice și aplicații.

Cuvinte cheie: nanofire semiconductoare, efecte dimensionale, izolator topologic, anizotropie, magnetorezistență, tranziții electronice

1. Introduction

For many years, $\text{Bi}_{1-x}\text{Sb}_x$ alloys have attracted the attention of researchers due to the fact that, on the one hand, these alloys can be used as a model material, which is extremely sensitive to stoichiometry, magnetic field, size, temperature, and deformations [1–3], and, on the other hand, these alloys are a promising material for thermoelectric energy converters at temperatures of 200 K, millivolt electronics, and infrared applications [4, 5].

$\text{Bi}_{1-x}\text{Sb}_x$ alloys are representatives of the semimetal–semiconductor band inversion semiconductor system. The general scheme of the energy spectrum restructuring in $\text{Bi}_{1-x}\text{Sb}_x$ alloys in a range of $0.05 < x < 0.22$ is shown in Fig. 1 [6].

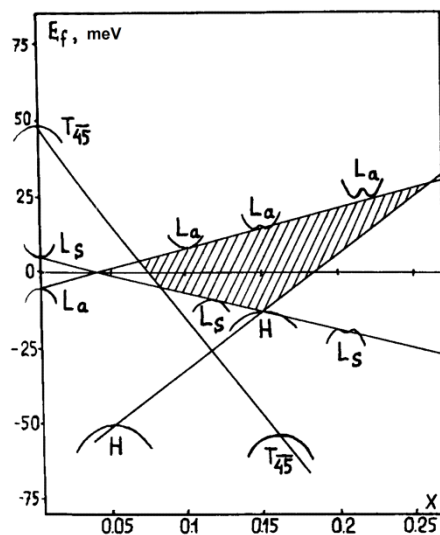


Fig. 1. Schematic rearrangement of the band structure of $\text{Bi}_{1-x}\text{Sb}_x$ as a function of x ($0 \leq x \leq 0.25$) at 4.2 K [6].

Recently, interest in objects based on $\text{Bi}_{1-x}\text{Sb}_x$ alloys has increased due to the development of new directions in basic solid state physics, namely, the discovery of a new class of materials—topological insulators (TIs) [7, 8] and low-dimensional structures based on TIs [9, 10]—in which, according to theoretical developments, an increase in the thermoelectric figure of merit is expected [11, 12]. Surface states within a bulk band gap with a linear dispersion law have been first experimentally observed in $\text{Bi}_{1-x}\text{Sb}_x$ semiconductor alloys using angle-resolved photoemission spectroscopy [13].

The authors of [14, 15] discuss the possibility of using TIs in next-generation electronic and spintronic devices; the predicted increase in thermoelectric figure of merit in low-dimensional TI structures makes it possible to use them to design alternative energy sources and miniature thermocooling devices.

In this manuscript, results of studying the electron transport and the manifestation of classical and quantum size effects in the longitudinal and transverse magnetoresistance (MR) of TI semiconductor wires of $\text{Bi}_{0.92}\text{Sb}_{0.08}$ alloys in a wide range of temperatures, magnetic fields, and wire diameters are described.

2. Experimental

Glass-insulated $\text{Bi}_{0.92}\text{Sb}_{0.08}$ semiconductor single-crystal wires with various diameters (0.15–2.2 μm) were prepared by liquid phase casting in accordance with the Ulitovsky method [16, 17]. All samples had a strictly cylindrical shape with a circular cross section, as confirmed by images in a scanning electron microscope [17, 18].

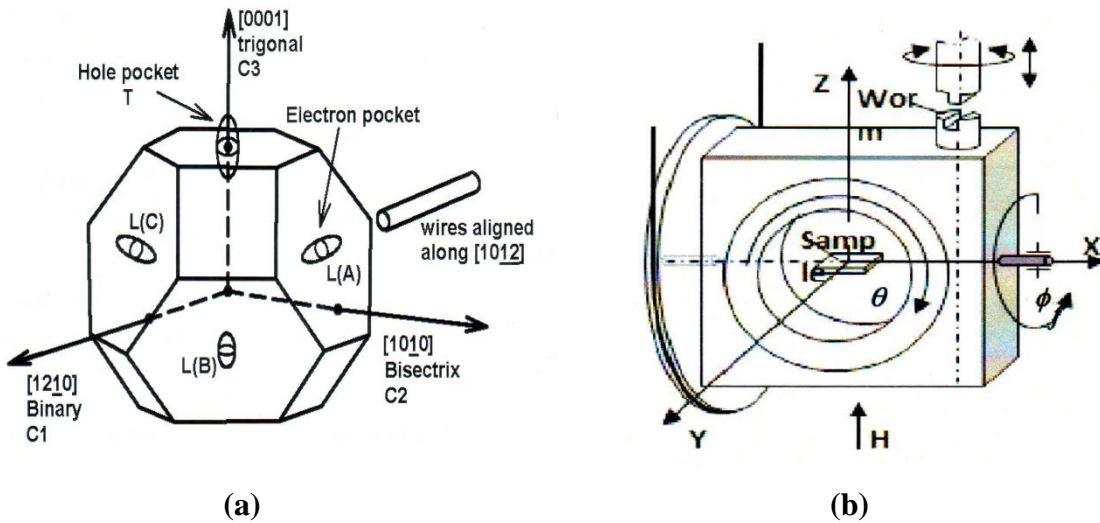


Fig. 2. (a) Reduced Brillouin zone of Bi with the hexagonal packing and the (1011) orientation of the $\text{Bi}_{1-x}\text{Sb}_x$ wires prepared by the Ulitovsky method and (b) a rotating device providing the rotation of a sample in two planes in the magnetic field of a superconducting solenoid.

The monocrystallinity and crystallographic orientation of $\text{Bi}_{0.92}\text{Sb}_{0.08}$ wires were detected by X-ray diffraction studies (X-ray diffraction diagrams of rotation). The $\text{Bi}_{0.92}\text{Sb}_{0.08}$ wires, in

common with pure Bi wires [17] and Bi–17at%Sb alloy wires prepared by a similar method [18, 19], were monocrystalline and had an identical orientation along the wire axis, namely, the (1011) orientation, at which the C_1 bisector axis is deviated from the wire axis by 20° , while the C_2 binary axis is strictly perpendicular to the wire axis (Fig. 2).

In the case of this crystallographic orientation of the wires, the direction of elongation of one electronic ellipsoid makes an angle of $\approx 20^\circ$ with the wire axis, the cross section of this ellipsoid S_1 with the plane perpendicular to the wire axis is close to minimal; the other two ellipsoids are localized symmetrically relative to the wire axis, and their cross section $S_{2,3}$ with the plane perpendicular to the wire axis is $S_{2,3} = 2S_1$ [18].

The measurements were conducted by a two-contact method using an InGa eutectics. The ohmicity of the contacts was verified by recording current–voltage characteristics in a temperature range of 4.2–300 K.

The rotation diagrams of the transverse MR and magnetic field dependences in perpendicular ($H \perp I$) and parallel magnetic fields were studied in the field of a superconducting solenoid in magnetic fields of up to 14 T at temperatures of 4.2–300 K using a special rotating device (Fig. 2b).

3. Results and Discussion

Figures 3 and 4 show the rotation diagrams of transverse MR of Bi–8at%Sb wires with different diameters (Fig. 3a), at different magnetic field H values (Figs. 3b, 4b), and at different temperatures (Fig. 4a). Point A corresponds to $H \parallel C_2$, while point B ($H \perp C_2$) corresponds to the direction deviated from the trigonal axis by 20° in the bisector–trigonal plane (Fig. 2a). The structures of the rotation diagrams of transverse MR for different diameters are identical and coincide with similar dependences of bulk samples [20]; this fact confirms that the studied wires have an identical crystallographic orientation.

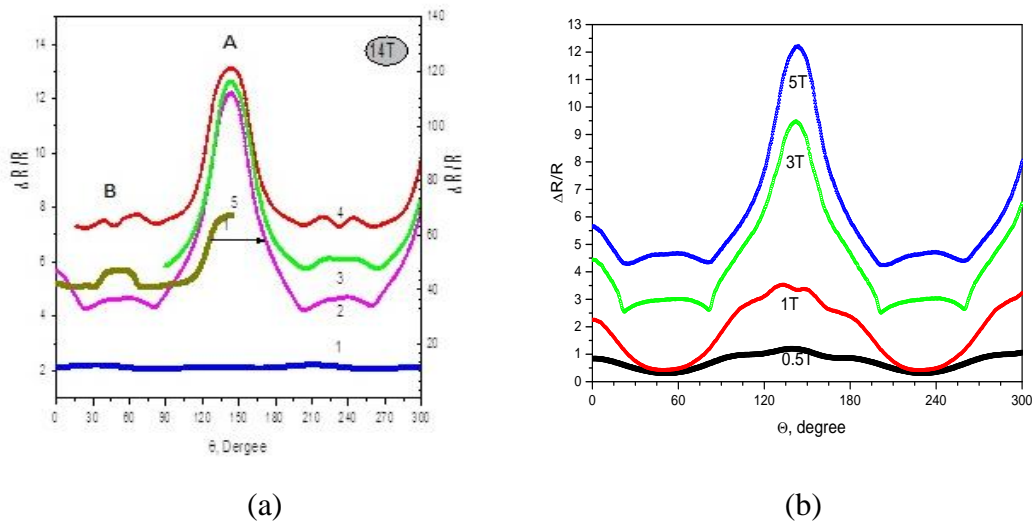


Fig. 3. (a) Rotation diagrams of transverse MR ($H \perp I$) of the $\text{Bi}_{0.92}\text{Sb}_{0.08}$ wires at 4.2 K, $H_{\perp} = 14$ T: $d = (1)$ 0.18, (2) 0.39, (3) 0.5, (4) 0.55, and (5) 2.2 μm (y-axis scale on the right outside) and (b) rotation diagrams of transverse MR $\Delta R/R(\theta)$ of the $\text{Bi}_{0.92}\text{Sb}_{0.08}$ wire at $d = 0.5$ μm , $T = 4.2$ K, and the different magnetic field H values.

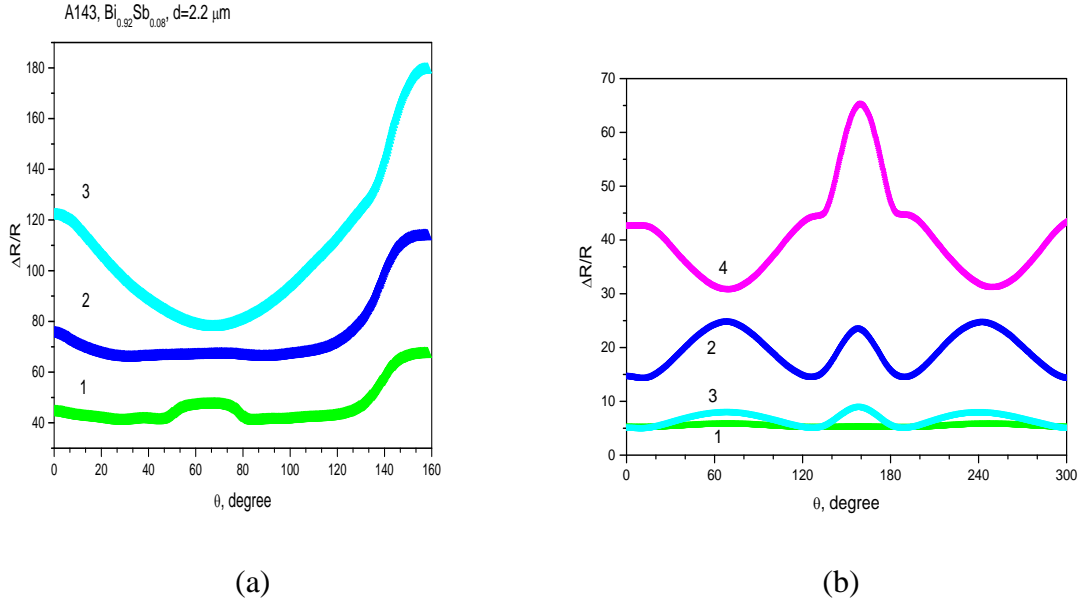


Fig. 4. Rotation diagrams of transverse MR $\Delta R/R(\theta)$ of the $\text{Bi}_{0.92}\text{Sb}_{0.08}$ wire at $d = 2.2 \mu\text{m}$ in a magnetic field of $H = 14 \text{ T}$ (a) at temperatures of $T = (1) 4.2$, (2) 50, and (3) 100 K and (b) at 100 K in magnetic fields of $H = (1) 0.1$, (2) 0.5, (3) 1, and (4) 5 T.

Figure 3a shows the rotation diagrams of transverse MR $\Delta R/R(\theta)$ at $H \perp I$ of Bi–8at%Sb wires with the different diameters in a magnetic field of 14 T at a temperature of $T = 4.2 \text{ K}$. It was found that the MR anisotropy ($A = R_{H||C2} / R_{H||C3}$) at 14 T and $T = 4.2 \text{ K}$ increases with a decrease in the wire diameter d from the value of $A = 1.4$ for the wire with $d = 2.2 \mu\text{m}$ to $A = 2.5$ for wires with $d = 0.39 \mu\text{m}$. The transverse MR anisotropy of the wire with $d = 2.2 \mu\text{m}$ at different temperatures in a magnetic field of $H = 14 \text{ T}$ (Fig. 3b) is maximal ($A = 2.3$) at 100 K (curve 3); at 4.2 K, $A = 1.4$. An increase in the magnetic field up to 5 T leads to a 1.5-fold decrease in anisotropy (Fig. 4b) in the Bi–8at%Sb wires with $d = 0.55 \mu\text{m}$. This anomalous change in the transverse MR anisotropy is a consequence of the semiconductor–semimetal electronic transition associated with the overlapping of the electron L_a and hole $T_{4,5}$ extremes in strong magnetic fields [21, 22].

3.1. Temperature dependence of resistance

Figure 5 shows temperature dependences of the reduced resistance $R_T/R_{300}(T)$ of $\text{Bi}_{0.92}\text{Sb}_{0.08}$ wires with different diameters in a temperature range of 4.2–300 K. At 300 K, the resistivity is almost independent of wire diameter d and has the same value as the resistivity of bulk single crystals $\rho_x = 145 \times 10^{-6} \Omega \text{ cm}$ [20].

The $\log_p(1/T)$ dependences show clear exponential portions $\rho_T = \rho_0 \cdot \exp(\Delta E/2k_0T)$, whose slope and region of existence depend on wire diameter d (Fig. 5, top inset).

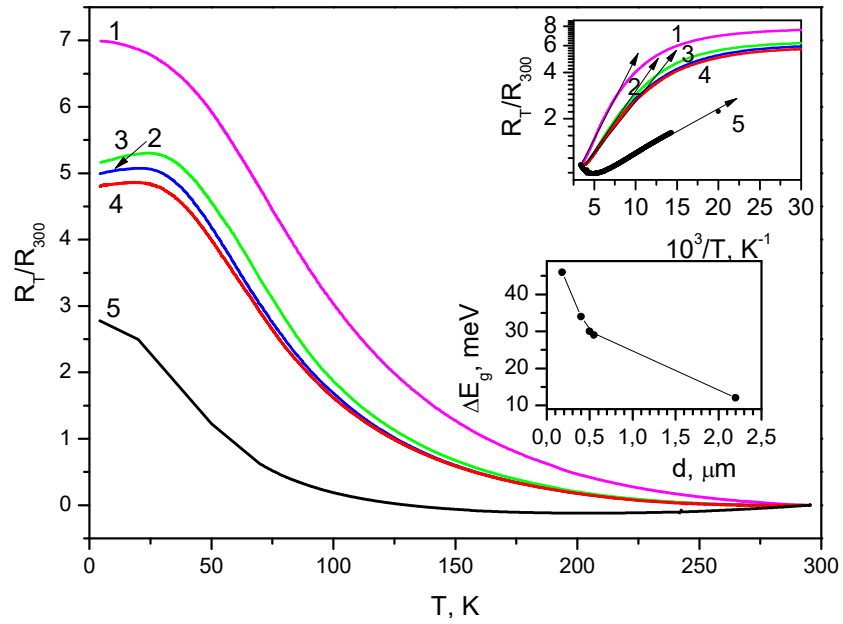


Fig. 5. Temperature dependences of the relative resistance $R_T/R_{300}(T)$ for $\text{Bi}_{0.92}\text{Sb}_{0.08}$ wires with diameters $d = (1) 0.18, (2) 0.39, (3) 0.5, (4) 0.55,$ and $(5) = 2.2 \mu\text{m}$. The top inset shows the $\ln \rho(T^{-1})$ dependence; the bottom inset shows the dependence of the energy gap ΔE on wire diameter d .

For the wires with $d \approx 2.2 \mu\text{m}$, the ΔE value determined from analysis of the $\ln \rho(T^{-1})$ dependences (curve 5) was 11–12 meV, which is in good agreement with the value for bulk samples. It was shown [21, 22] that, in semiconductor alloys $\text{Bi}_{1-x}\text{Sb}_x$ with $0.07 < x < 0.09$, the minimum energy gap is the ΔE_{LT} indirect gap (Fig. 1) equal to the distance between the conduction band bottom at point L of the Brillouin zone and the valence band top at point T. With a decrease in wire diameter d , the energy gap increases; this fact is associated with the manifestation of the quantum size effect [9, 10].

It has been first found that, with a decrease in wire diameter d , the energy gap ΔE increases almost fourfold and achieves a value of 47 meV in the wires with $d \approx 180 \text{ nm}$. In similar Bi–17at%Sb wires, the energy gap ΔE_g increases about twofold at significantly smaller diameters ($d = 75 \text{ nm}$) [19].

The dependence of the energy gap $\Delta E \sim d^{-1}$ (Fig. 5, inset) indicates that the cause of the increase in ΔE with a decrease in the wire diameter d is the quantum size effect predicted in [9] and observed in Bi, Bi–2at%Sb, and Bi–17at%Sb wires [17, 19, 23].

This significant increase in the energy gap can be attributed to the fact that, according to [7, 13], near the gapless state, the dispersion law differs from the quadratic law and becomes similar to the "Dirac-type" law characterized by a linear energy–momentum dependence $E = \hbar k v_F$, where v_F is the Fermi velocity of electrons. This factor leads to a more significant shift of the energy bands due to the quantum size effect and an increase in the gap to 47 meV.

Therefore, unlike Bi–17at%Sb wires, the surface states characteristic of TIs do not lead to this abrupt decrease in the resistance and metallic conductivity at temperatures of $T < 50 \text{ K}$.

3.2. Magnetoresistance

Both longitudinal ($H \parallel I$) and transverse ($H \perp I$) MR was studied ($H \parallel C_2$ and $H \perp C_2$) in magnetic fields of up to 14 T at $T = 4.2\text{--}100$ K. Figure 6 shows the field dependences of the longitudinal MR for Bi–8%Sb wires with different diameters at $T = 4.2$ K in magnetic fields of up to 14 T. In the $MR(H) = \Delta U/U = \Delta R/R = (R_H - R_0)/R_0$ field dependences of relative MR, three regions of longitudinal MR can be distinguished: an abrupt increase in the resistance in weak magnetic fields, the formation of a maximum, and a decrease in the resistance with the formation of a region of negative MR in strong magnetic fields.

The dependence of $H_{\max} \sim d^{-1}$ (inset in Fig. 7) and the subsequent negative MR indicate the occurrence of the galvanomagnetic size effect (MacDonald–Chambers) [24], which is observed in pure bismuth wires [16, 17]. The initial increase in the resistance of the wires in a longitudinal magnetic field is attributed to the fact that the distortion of the trajectory of charge carriers by a magnetic field leads to a decrease in the mobility due to the contribution of surface scattering.

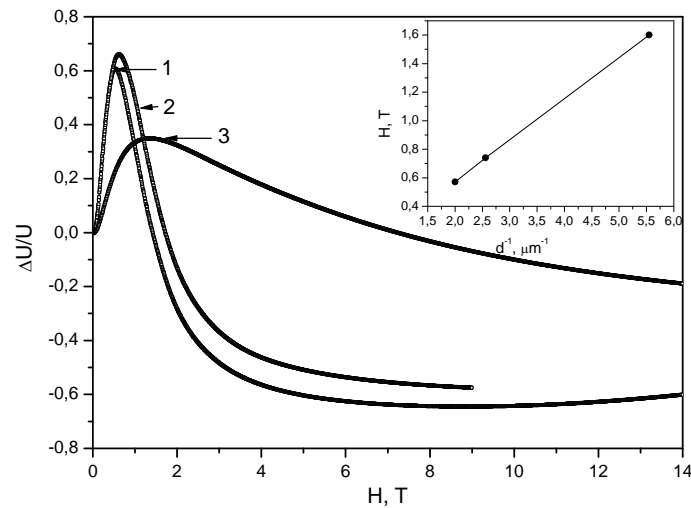


Fig. 6. Field dependences of the relative longitudinal MR $\Delta U/U = \Delta R/R = (R_H - R_0)/R_0$ at 4.2 K for $\text{Bi}_{0.92}\text{Sb}_{0.08}$ wires with $d = (1)$ 0.18, (2) 0.39, and (3) 0.55 μm .

In the region where the Larmor radius r_L is equal to the wire diameter d ($r_L = d$), the role of the surface is excluded and the resistance decreases with an increase in magnetic field H . The shift of the maximum in $R(H)$ to the region of stronger magnetic fields with a decrease in wire diameter d is attributed to an increase in the magnetic field magnitude for the fulfillment of the condition $r_L = d$ (Larmor radius fits into the cross section of the cylinder), $r_L = p_F^\perp \cdot c/e \cdot H$, where p_F^\perp is the component of the Fermi momentum perpendicular to the magnetic induction vector H . The value of $P_F = 4.0 \times 10^{-21}$ g/(cm s) calculated for Bi–8%Sb wires is 2 times higher than the value in pure Bi wires [16, 17]; this fact is apparently associated with the manifestation of the quantum size effect in 1D TIs [11, 13]. The R_H/R_0 value at the maximum point decreases with an increase in wire diameter d , as in pure Bi wires and in Bi–17at%Sb semiconductor wires,

in a diameter range of 75–200 nm [19].

The transverse MR $R(H)$ ($H \perp I$) was studied at points *A* and *B* (Fig. 3) in magnetic fields of up to 14 T at different temperatures. Figures 7 and 8 show the field dependences of the relative MR $R_H/R_0(H)$ at points *A* and *B* corresponding to $H \parallel C_2$ and $H \parallel C_3$ in the rotation diagrams of transverse MR in magnetic fields of 14 T at temperatures of $T = (1)$ 4.2, (2) 20, (3) 54, (4) 72, and (5) 100 K.

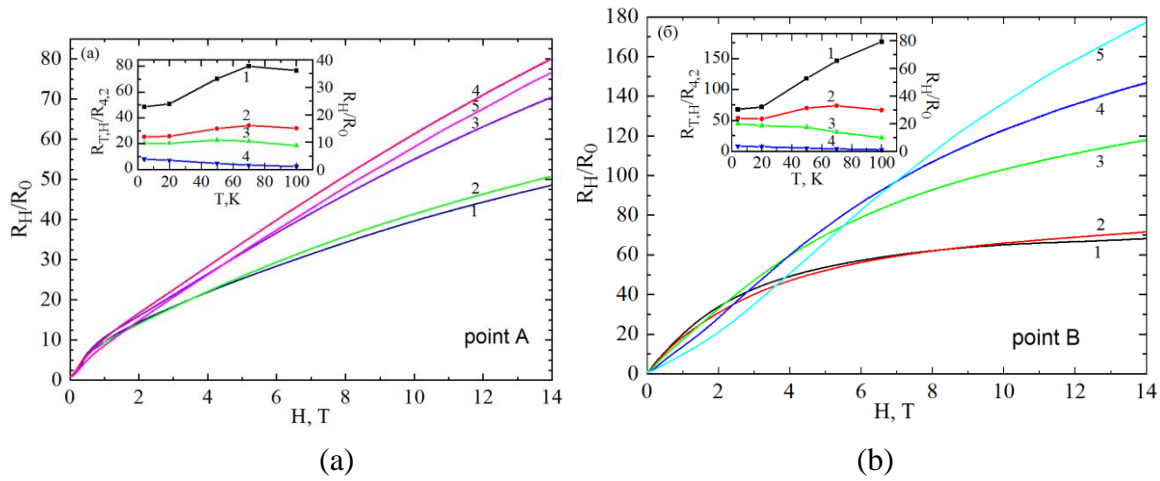


Fig. 7. Field dependences of the relative transverse MR $R_H/R_0(H)$ of the $\text{Bi}_{0.92}\text{Sb}_{0.08}$ wire with $d = 2.2 \mu\text{m}$ at the different temperatures: $T = (1)$ 4.2, (2) 20, (3) 54, (4) 72, and (5) 100 K; (a) $H \parallel C_2$ and (b) $H \parallel C_3$ (points *A* and *B* in the angular rotation diagram). The insets show temperature dependences of resistance $R_{T,H}/R_{4,2}(T)$ in a magnetic field of $H = (1)$ 14, (2) 5, (3) 1, and (4) 0 T (for curves 3 and 4, scale on the right).

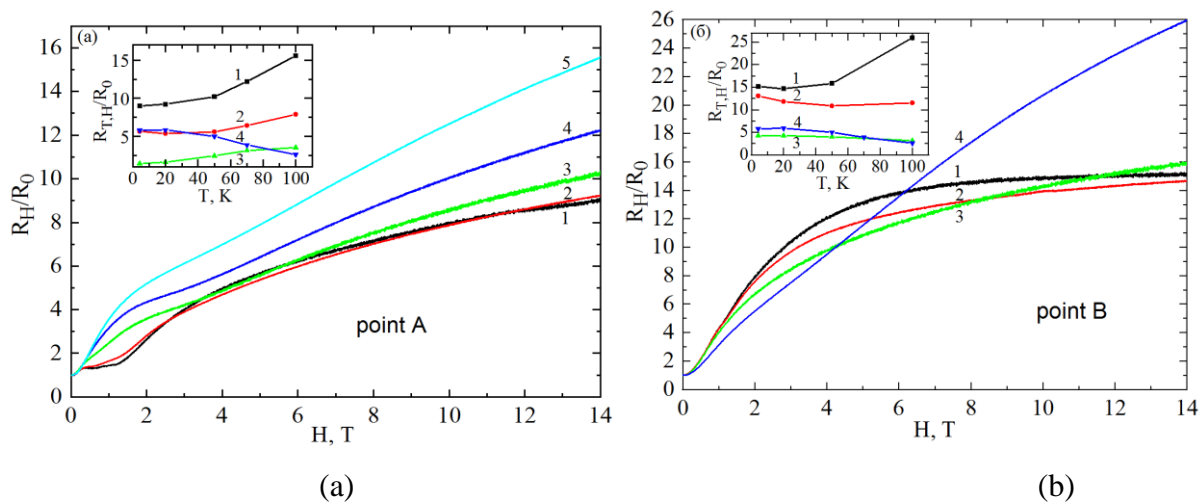


Fig. 8. Field dependences of the relative transverse MR $R_H/R_0(H)$ of the $\text{Bi}_{0.92}\text{Sb}_{0.08}$ wire with $d = 0.55 \mu\text{m}$ at different the temperatures: (a) $H \parallel C_2$ and (b) $H \parallel C_3$. The insets show temperature dependences of resistance $R_{T,H}/R_{4,2}(T)$ in a magnetic field of $H = (1)$ 14, (2) 5, (3) 1, and (4) 0 T.

In weak magnetic fields ($H < 2$ T), a monotonic increase in MR with an increase in the magnetic field at $H \parallel C_2$ and at $H \parallel C_3$ is observed, while the relative MR R_H/R_0 at 4.2 K is higher than that at 100 K. However, in strong magnetic fields ($H > 3$ T), the behavior of the curves qualitatively changes: the relative MR $R_{14T}/R_0(H)$ at 4.2 K becomes lower than that at 100 K; at $H \parallel C_3$, it tends to saturation in magnetic fields of >3 T (Figs. 7, 8, curves 1, 2), because the current carrier mobility decreases in a magnetic field.

The saturation and decrease in the resistance $R_{14T}/R_0(H)$ in strong magnetic fields at low temperatures in $\text{Bi}_{1-x}\text{Sb}_x$ semiconductor wires can be observed only upon this rearrangement of the energy spectrum in a quantizing magnetic field, at which the charge carrier concentration increases. An increase in the concentration of electrons and holes in $\text{Bi}_{0.92}\text{Sb}_{0.08}$ wires in strong magnetic fields at $H \parallel C_3$ is a consequence of the semiconductor–semimetal electronic transition induced by a strong magnetic field and caused by the overlapping of the electron L and hole T extremes [21, 22].

At low temperatures, in the direction of the quantizing magnetic field along C_3 , the L-terms converge, and the hole extreme at point T of the momentum space rises up the energy scale; as a result, the direct ΔE_L and indirect ΔE_{LT} gaps decrease and can overlap. The insets to Figs. 7 and 8 (a, b) show the temperature dependences $R_H/R_0(T)$ in a magnetic field (curves 1–3) and $R_T/R_{4.2}(T)$ without a magnetic field (curve 4) in the region of $T = 4.2\text{--}100$ K for $\text{Bi}_{0.92}\text{Sb}_{0.08}$ wires with two different diameters d at points A and B. It is evident from the figures that the temperature dependences exhibit a "metallic" behavior (curves 1, 2 in the insets). At $T < 100$ K, the resistance decreases by a factor of 2.6 in the wires with $d = 2.2$ μm , for which the gap is minimal (≈ 11 meV), whereas in the absence of a magnetic field, the $R(T)$ dependence exhibits a semiconductor behavior (curves in the insets). In thinner wires, the effect of the semiconductor–semimetal transition is less pronounced (curves 2–4).

A similar effect in semiconductor alloys in a strong magnetic field was observed in bulk samples of BiSb alloys doped with Te [25].

Thus, a strong magnetic field leads to the occurrence of semiconductor–semimetal topological transitions in $\text{Bi}_{1-x}\text{Sb}_x$ semiconductor wires at low temperatures; in thin wires, stronger magnetic fields are required for the occurrence of the effect.

4. Conclusions

A comprehensive study of the resistance and longitudinal and transverse MR in $\text{Bi}_{0.92}\text{Sb}_{0.08}$ single-crystal wires with different diameters in a temperature range of 4.2–300 K and magnetic fields of up to 14 T has been conducted. It has been found that the manifestation of the quantum size effect in TI wires based on $\text{Bi}_{0.92}\text{Sb}_{0.08}$ alloys leads to an increase in the energy gap by a factor of 4 with a decrease in the wire diameter to 180 nm; this finding is attributed to a linear dispersion law in TIs. In a longitudinal magnetic field, the classical size effect of negative MR depending on wire diameter d is observed. In transverse magnetic fields, semiconductor–semimetal electronic transitions have been detected; they lead to a decrease in the MR anisotropy in strong magnetic fields and a metallic temperature dependence of the resistance at a temperature of $T < 100$ K.

Acknowledgments. This work was financially supported by the State Program of the Ministry of Education, Culture, and Innovation of the Republic of Moldova (project no. 20.80009.5007.02)

and the following American funds: NSF through STC CIQM 1231319, the Boeing Company, and the Keck Foundation.

References

- [1] S. Golin, *Phys. Rev.* 176 (3), 830 (1968).
- [2] N. B. Brandt, M. V. Semenov, and L. A. Falkovsky, *J. Low Temp. Phys.* 27, 75 (1977).
- [3] G. A. Mironova, M. V. Sudakova, and Ya. G. Ponomarev, *Zh. Eksp. Teor. Fiz.* 76 (5), 1832 (1980).
- [4] M. S. Dresselhaus, Yu. M. Lin, T. Koga, S. B. Cronin, O. Rabin, M. R. Black, and G. Dresselhaus, Recent Trends in Thermoelectric Materials Research 111, in *Semiconductors and Semimetals*, Ed. by T. M. Tritt (Academic, San Diego, 2001, pp. 1–121).
- [5] L. I. Anatyshuk, *Thermoelements and Thermoelectric Devices: Reference Book* (Naukova Dumka, Kyiv, 1979).
- [6] L. S. Lerner, F. Cuff, and L. N. Williams, *Rev. Mod. Phys.* 40 (4), 770 (1968).
- [7] Fu Liang and C. L. Kane, *Phys. Rev. B* 76, 045302 (2007).
- [8] J. E. Moore, *Nature* 464, 194 (2010).
- [9] Shuang Tang and Mildred S. Dresselhaus, *Phys. Rev. B* 89, 045424 (2014).
- [10] Jane E. Cornett and Oded Rabin, *Appl. Phys. Lett.* 98, 182104 (2011).
- [11] Ryuji Takahashi and Shuichi Murakami, *Nature* 460, 1101 (2009).
- [12] O. Rabin, Y. M. Lin, and M. S. Dresselhaus, *Appl. Phys. Lett.* 79, 81 (2001).
- [13] D. Hsieh et al., *Nature* 460, 1101 (2009).
- [14] Shuang Tang and Mildred S. Dresselhaus, *Nano Letters* 12 (4), 2021 (2012).
- [15] X. L. Qi, R. Li, J. Zang, and S. C. Zhang, *Science* 323 (5918), 1184-7 (2009).
- [16] N. B. Brandt, D. V. Gitsu, A. A. Nikolaeva, and Ya. G. Ponomarev, *JETP* 45 (6), 1226 (1977).
- [17] A. Nikolaeva, T. E. Huber, D. Gitsu, and L. Konopko, *Phys. Rev. B* 77 (3), 035422 (2008).
- [18] L. A. Konopko, A. A. Nikolaeva, and T. E. Huber, *J. Low Temp. Phys.* 185 (5), 673 (2016).
- [19] Leonid Konopko, Albina Nikolaeva, Tito E. Huber, and Krzysztof Rogacki, *Appl. Surf. Sci.* 526, 146750 (2020).
- [20] A. A. Taskin, Kouji Segawa, and Yoichi Ando, *Phys. Rev. B* 82, 121302(R) (2010).
- [21] N. B. Brandt, E. A. Svistova, and R. G. Valeev, *Zh. Eksp. Teor. Fiz.* 55 (8), 469 (1968).
- [22] W. E. Fenton, J.-P. Jan, and A. Karlsson, *J. Low Temp. Phys.* 3 (2), 147 (1970).
- [23] A. A. Nikolaeva, L. A. Konopko, T. E. Huber, J.-Ph. Ansermet, and, I. A. Popov, *J. Nanoelectron. Optoelectron.* 7 (7), 671 (2012). DOI: <http://dx.doi.org/10.1166/jno.2012.1414moja-2-Sb>
- [24] R. G. Chambers, *Proc. R. Soc.* 202, 378 (1950).
- [25] N. A. Red'ko and N. A. Rodionov, *Pis'ma Zh. Eksp. Teor. Fiz.* 42 (6), 246 (1985).